

Probing phase coupling between two spin-torque nano-oscillators with external source

Yi Li,^{1,*} Xavier de Milly,¹ Flavio Abreu Araujo,² Olivier Klein,³

Vincent Cros,² Julie Grollier,² and Grégoire de Loubens^{1,†}

¹*Service de Physique de l'État Condensé, CEA, CNRS, Université Paris-Saclay, Gif-sur-Yvette, France*

²*Unité Mixte de Physique CNRS, Thales, Univ. Paris-Sud, Université Paris-Saclay, Palaiseau, France*

³*SPINTEC, Univ. Grenoble Alpes / CEA / CNRS, 38000 Grenoble, France*

(Dated: May 9, 2022)

Phase coupling between auto-oscillators is central for achieving coherent responses such as synchronization. Here we present an experimental approach to probe it in the case of two dipolarly coupled spin-torque vortex nano-oscillators using an external microwave field. By phase-locking one oscillator to the microwave field, we observe frequency pulling on the second oscillator. From coupled Thiele equations we show analytically that this frequency pulling results from concerted actions of dipolar and microwave couplings. The analysis allows us to determine the amplitude of dipolar coupling and the phase lag of each oscillator, yielding important information for the implementation of large oscillator networks.

INTRODUCTION

Self-sustained oscillators which are linked by phase coupling exhibit abundant collective dynamics[1] and describe diverse systems in nature[2–10]. In particular, they can synchronize, which is important in the fields of engineering, biology and computing. Indeed, synchronizing oscillators allows improving the amplitude and spectral purity of their outputs, and can be used to study and mimic neural networks[11, 12]. Theoretical explorations of this phenomenon have been ongoing for decades in particular within the framework of the Kuramoto model[13, 14], where phase coupling is simplified as a sinusoidal function of phase difference. In experiments, technology progress has allowed mutual synchronization in many systems compatible with lithographic fabrications, such as Josephson junctions[2], nanomechanical and optomechanical structures[3–5], and spin-torque nano-oscillators[6, 7, 15–18]. Despite those successes, the knowledge of the inter-device coupling remains to be extended. Notably, besides coupling strength, the relative phase shift between oscillators also determines the occurrence of synchronization[19, 20].

Among different oscillator systems, spin-torque nano-oscillators[21] serve as outstanding candidates for implementing coupled oscillator arrays, due to their sub-micron dimensions, nonlinear behaviors with large frequency tunability, simple signal extractions from magnetoresistance and ease to be coupled and synchronized[6, 7, 15–18, 22–27]. Of special engineering interests are spin-torque vortex oscillators (STVOs)[28, 29] which allow operations without biasing field and different tuning properties linked to vortex polarity[30–32]. The synchronization of two adjacent STVOs through their dipolar field[33–35] has been demonstrated[17, 36–38], as well as the control of the phase-locking bandwidth by their relative vortex polarities[17, 39]. This is important for coupled-oscillator-based associative memories proposed recently, where controlling the coupling between neigh-

boring oscillators is a prerequisite as it is the support of information[40, 41].

In this work we add a third “oscillator”, namely, a microwave field with tunable frequency and power, to a pair of dipolarly coupled STVOs. By adjusting the frequency so that the microwave field phase-locks one STVO, an obvious frequency pulling is measured on the second STVO. In the limit of weak microwave field, we show from coupled Thiele equations that this frequency pulling is due to in-phase actions of dipolar and microwave forces within the phase-locking bandwidth, beyond which it disappears. The model is tested by varying both the microwave power and the dipolar coupling strength. Fittings at different powers yield consistent amplitude of dipolar coupling and phase lag of each oscillator for antiparallel polarity alignment. Changing to parallel polarity alignment yields a 2.2 times weaker dipolar coupling strength, in agreement with prior theories and experiments[17, 39]. Our results provide a new way to fully characterize the mutual coupling between oscillators, which can be applied to various oscillator systems.

EXPERIMENTS

Our sample consists of two cylindrical spin-torque nano-oscillators with identical nominal geometry of 400 nm in diameter, shown in Fig. 1(a). Each oscillator has a spin-valve layer structure of Py(15 nm)/Cu(10 nm)/Py(4 nm) (Py = Ni₈₀Fe₂₀). During the operations a dc current of 95 mA is injected through the two oscillators in parallel, corresponding to 1.5 times the critical current for auto-oscillation. The two Py layers in each oscillator are in vortex states with the same chirality[42], which is imposed by the direction of the injected dc current through the in-plane curling Oersted field it generates. The sign of current is set to induce auto-oscillations of the thick Py layers in each device[43]. The two oscillators have an edge-to-edge separation of 200 nm in order to allow

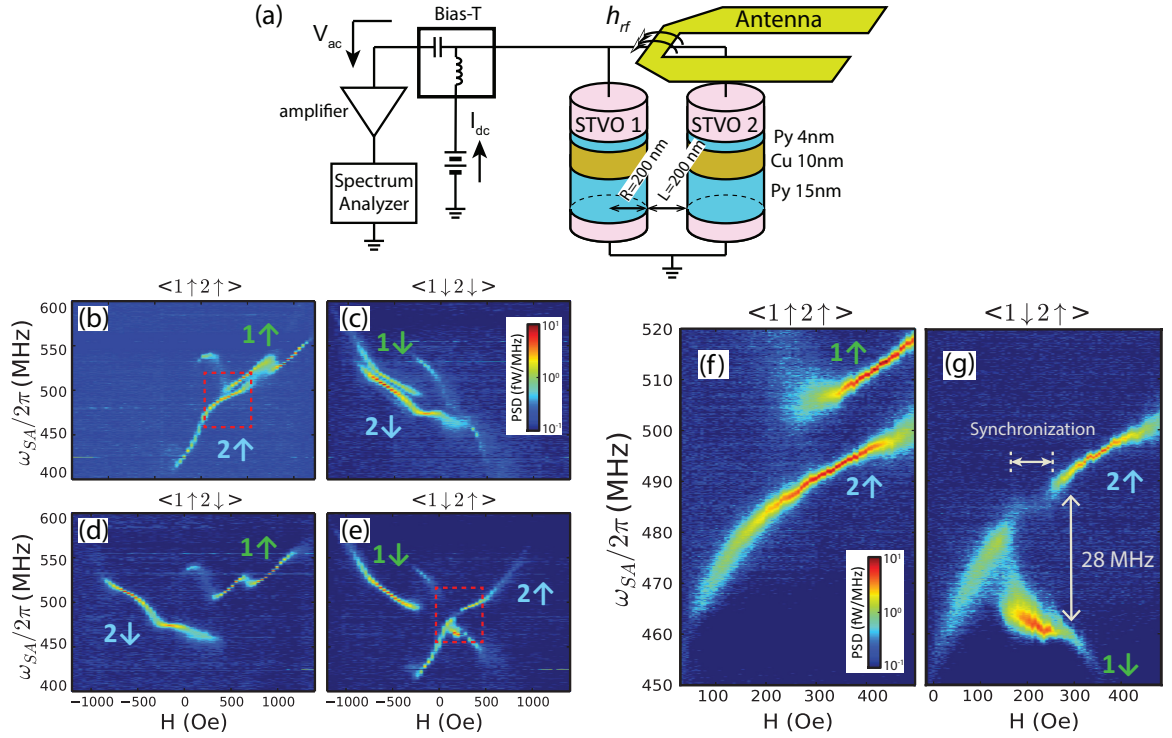


FIG. 1. (a) Schematics of the sample and electrical circuit. (b-g) Power spectral density maps of auto-oscillation modes in log scale. Four different polarity states of the two thick Py vortex layers are shown: (b) $\langle 1 \uparrow 2 \uparrow \rangle$, (c) $\langle 1 \downarrow 2 \downarrow \rangle$, (d) $\langle 1 \uparrow 2 \downarrow \rangle$ and (e) $\langle 1 \downarrow 2 \uparrow \rangle$. The background has been subtracted. (f,g) Zoomed-in power spectral density data of $\langle 1 \uparrow 2 \uparrow \rangle$ and $\langle 1 \downarrow 2 \uparrow \rangle$ for the red box regions of (b) and (e), respectively. Mutual synchronization is observed between $H = 175$ and 260 Oe in $\langle 1 \downarrow 2 \uparrow \rangle$ state.

strong dipolar coupling[17]. To provide an external rf field, an antenna is patterned on top of the sample[44] creating an in-plane h_{rf} linearly polarized along the direction made by the two STVOs (see Fig. 1a). Furthermore a biasing magnetic field is applied perpendicular to the sample plane in order to change the gyrotropic frequencies[45, 46]. The ac signal output is filtered by a bias-T, amplified, and then detected using a spectrum analyzer.

RESULTS AND ANALYSIS

First we demonstrate the microwave signal associated with auto-oscillations in each STVO. Figs. 1(b-e) show the colored maps of the power spectral density as a function of perpendicular field for all four different polarity states, obtained after applying well-chosen perpendicular switching fields[30]. Two branches are observed in each case which correspond to the gyrotropic modes of the thick layer vortex in each device. The field dependence in each branch follows $\omega(H)/\omega(0) = 1 + pH/H_s$ where $\omega(0)$ is the auto-oscillation frequency at zero biasing field, H_s is the perpendicular saturation field and p is the vortex core polarity which determines the sign of ω - H slope[45, 46]. Estimation of $\omega(0)$ using analyti-

cal formulae[46, 47] confirms that the spin-torque driven dynamics is dominated by the gyrotropic modes in the thick Py layers.

Next we show the existence of dipolar coupling by the observation of mutual synchronization. Figs. 1(f,g) compare the zoomed-in power spectra of $\langle 1 \uparrow 2 \uparrow \rangle$ and $\langle 1 \downarrow 2 \uparrow \rangle$ states for $0 \leq H \leq 500$ Oe, as labeled by the red boxes in Figs. 1(b) and (e), respectively. By switching the polarity of STVO 1, a clear gap of the auto-oscillation branch for STVO 2 is found between $H = 175$ and 260 Oe in $\langle 1 \downarrow 2 \uparrow \rangle$ state, while for $\langle 1 \uparrow 2 \uparrow \rangle$ state the branch is continuous. This gap, accompanied by a bright lower-frequency branch, is associated to the synchronization of the two STVOs. From the right edge of the synchronization bandwidth we deduce that the maximal frequency mismatch for mutual synchronization is 28 MHz. The frequency mismatch corresponding to the unlocking of the two STVOs at the left edge is smaller. We attribute this to the fact that the amplitude of STVOs can vary with the perpendicular field[31], which will change the effective dipolar coupling. The results above show that the dipolar interaction is strong enough to synchronize the two STVOs. Still, a quantitative evaluation of its strength and locking phase is lacking at this point.

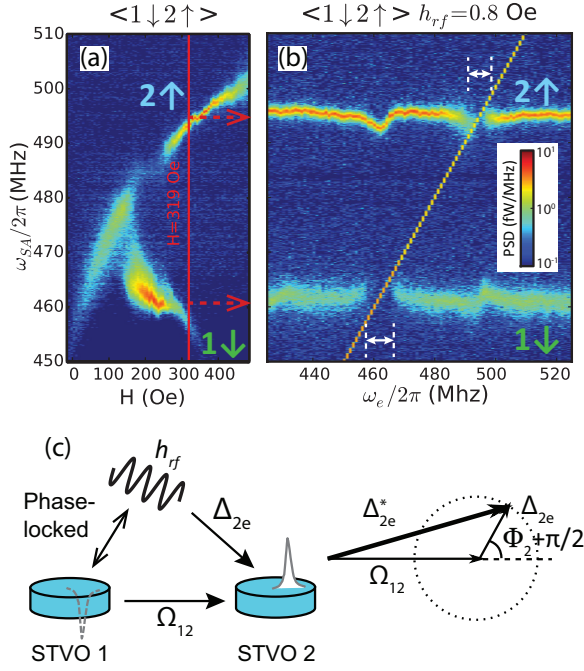


FIG. 2. (a) Location of spectra at $\langle 1 \downarrow 2 \uparrow \rangle$ state for the microwave study. (b) Auto-oscillation spectra as a function of microwave field frequency for $H = 319$ Oe, indicated in (a). Signal from the source appears as the oblique narrow line. The microwave power is -23 dBm, corresponding to $h_{rf} = 0.8$ Oe. White arrows show the phase-locking bandwidths. (c) Vector diagram of Ω_{12} and Δ_{2e} when STVO 1 is phase-locked to the microwave field.

In order to quantify the dipolar coupling, we fix both the biasing current and magnetic field and apply a weak microwave field, which couples to both STVOs. The two STVOs are set to an unsynchronized state at $H = 319$ Oe, shown in Fig. 2(a). Fig. 2(b) shows the evolution of auto-oscillation peaks of the two STVOs as a function of the external microwave field frequency ω_e . When ω_e crosses the STVO 1 peak around 460 MHz, the disappearance of the peak reflects the phase locking to the external rf source[22, 23, 26]. In addition, we also detect a significant frequency pulling on STVO 2. This is a striking observation, because the frequency mismatch between STVOs, $\omega_2 - \omega_1 = 35$ MHz, is five times larger than the phase-locking bandwidths, around 7 MHz, of the two STVOs to the external source. The remote frequency pulling is a strong indication of coupling between the two oscillators as it is bound to the phase-locking bandwidth. It is important to note that no obvious frequency shift is observed when ω_e lies between the two auto-oscillation peaks. Reciprocally, similar effect is also observed on STVO 1 when STVO 2 is phase-locked to the microwave field around 495 MHz.

To phenomenologically understand these phenomena, we develop a simplified analytical formalism based on general oscillator equations[48]. For two dipolarly

coupled vortex oscillators experiencing a linearly polarized microwave field, the phase equations can be formulated[42] from the Thiele equation which describes the vortex core dynamics in a magnetic dot[49–51], as:

$$\begin{aligned} -\frac{d\theta_i}{dt} + \omega_e - \omega_{ig} + \Omega_{ji} \cos(\theta_i + \gamma_i^{NL} - \theta_j) \\ - \Delta_{ie} \sin(\theta_i + \gamma_i^{NL} + \gamma_i^{rf}) = 0 \end{aligned} \quad (1)$$

where $\theta_i = \omega_e t + \varphi_e - p_i \varphi_i$ is the phase difference between the microwave field and the vortex core gyration, p_i is the vortex polarity, ω_e is the microwave frequency, ω_{ig} is the frequency of isolated STVO i , $\Omega_{ji} = \Omega(X_j/X_i)$ is the effective dipolar coupling strength normalized by the ratio of vortex gyration amplitudes X_j/X_i and Δ_{ie} is the coupling amplitude to the external microwave source. The index is defined as $(i, j) = (1, 2)$ or $(2, 1)$. In Eq. (1) two additional phases are present: γ_i^{rf} is determined by the geometric alignment of the microwave field to the device; γ_i^{NL} is the phase shift introduced by the nonlinearity of the oscillators[48]. We highlight that Eq. (1) describes the general behaviors of self-sustained oscillators: for $\Omega = 0$, it is reduced to the Adler equation responsible for one oscillator phase-locking to an external source [52]; for $\Delta_{ie} = 0$, it is reduced to Kuramoto equations in the case of two coupled oscillators[14].

When STVO 1 is phase-locked to the microwave field, the microwave coupling dominates in Eq. (1). Because the influence from dipolar coupling is determined by the frequency difference of the two STVOs, this term is assumed to be unchanged as long as the frequency pulling is much smaller than the devices frequency difference. The approximation agrees with the experimental observation that phase locking takes place around the oscillator frequency. The solution of θ_1 is then taken as:

$$\sin(\theta_1 + \gamma_1^{NL} + \gamma_1^{rf}) = \frac{\omega_e - \omega_{1g}^c}{\Delta_{1e}} \quad (2)$$

Here ω_{1g}^c is the frequency of STVO 1 in the presence of dipolar coupling, corresponding to the experimentally measured auto-oscillation peaks.

For STVO 2 a constant θ_1 due to phase locking gives rise to an Adler-like equation:

$$-\frac{d\theta_2}{dt} + \omega_e - \omega_{2g} = -\Delta_{2e}^* \sin(\theta_2 + \gamma_2^{NL} + \gamma_2^{rf} + \gamma^*) \quad (3)$$

where

$$\Delta_{2e}^* = \sqrt{\Delta_{2e}^2 + \Omega_{12}^2 - 2\Delta_{2e}\Omega_{12}\sin\Phi_2} \quad (4a)$$

$$\tan\gamma^* = \frac{\Omega_{12}\cos\Phi_2}{\Omega_{12}\sin\Phi_2 - \Delta_{2e}} \quad (4b)$$

The new frequency of STVO 2, solved from Eq. (3), is $\omega_2 = \omega_e + \text{sgn}(\omega_e - \omega_{2g})\sqrt{(\omega_e - \omega_{2g})^2 - (\Delta_{2e}^*)^2}$.

In Eq. (3) a new phase-locking amplitude, Δ_{2e}^* , acts as a frequency puller. It is the vector sum of the dipolar coupling Ω_{12} and the microwave coupling Δ_{2e} with a

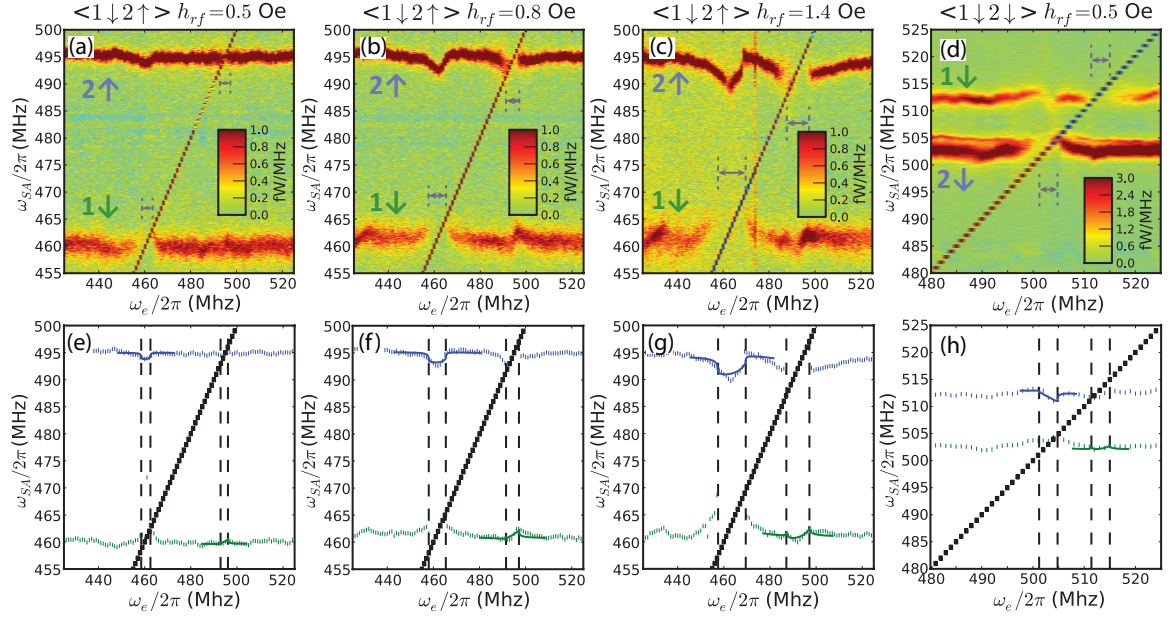


FIG. 3. Probing dipolar coupling at various conditions. (a-c) Antiparallel polarity state with microwave powers of (a) -28 dBm, (b) -23 dBm and (c) -18 dBm. The polarity state and the biasing field are the same as Fig. 2(b). (d) Parallel polarity state $<1 \downarrow 2 \downarrow>$ with biasing field $H = -616$ Oe. The grey arrows show the phase-locking bandwidths to the microwave field. The scale change is to facilitate identifications of phase-locking bandwidths. (e-h) Extracted peak positions from (a-d), respectively. Blue and green curves show the fits from the analytical model. The vertical dashed lines show the phase-locking bandwidths. The fit parameters are listed in Table I.

phase difference of $\Phi_2 + \pi/2$ where $\Phi_2 = \theta_1 + \gamma_2^{rf}$ (Fig. 2c). The additional phase of $\pi/2$ on θ_1 is due to fact that the direction of the dynamic magnetization is perpendicular to the vortex core displacement[42]. From Eq. (2) we can rewrite Φ_2 as:

$$\Phi_2(\omega_e) = \sin^{-1} \left(\frac{\omega_e - \omega_{1g}^c}{\Delta_{1e}} \right) - \gamma_1^{NL} + (\gamma_2^{rf} - \gamma_1^{rf}) \quad (5)$$

Importantly, from Eq. (5) the phase between the dipolar and microwave couplings on STVO 2 is shifted by γ_1^{NL} . For the antenna geometry used in this work, $\gamma_2^{rf} - \gamma_1^{rf} = \pi$ and 0 for antiparallel and parallel polarity alignments, respectively[42]. We also note that positive and negative signs of Ω are expected for parallel and antiparallel polarity alignments, respectively[39], which is taken into account in our fittings.

	antiparallel			parallel
h_{rf} (Oe)	0.5	0.8	1.4	0.5
$\frac{\Delta_{1e} + \Delta_{2e}}{2}$ (MHz)	1.8	3.2	5.5	1.8
Ω (MHz)	-6.7	-7.9	-9.3	3.6
γ_1^{NL} (rad)	-2.7	-2.8	-2.0	2.6
γ_2^{NL} (rad)	1.1	1.1	0.7	-2.1

TABLE I. Fit parameters of Fig. 3. The values of h_{rf} are calculated from the antenna geometry. The signs of Ω are fixed to the predictions in Ref. [39].

In Fig. 3 we use our model to extract the coupling

parameters from two different experiments. First, the microwave power of the external field is varied in the antiparallel polarity state (Figs. 3a-c), where we observe obvious frequency pulling with a frequency mismatch as large as 35 MHz. Second, the polarity alignment is changed from antiparallel to parallel (Fig. 3d), a case for which the dipolar coupling strength is expected to decrease by a factor close to three[17, 39]. Figs. 3(e-h) show the fitting curves to the model, reproducing the experiments reasonably within the phase-locking bandwidths. The fit parameters are Ω and γ_i^{NL} . In Ω_{ij} the amplitude ratio X_i/X_j accounts for the asymmetry of frequency pulling amplitudes in the two reciprocal cases. In the experiment we find the best amplitude ratio to be $X_1/X_2 = 1.1$ for the antiparallel polarity alignment and $X_1/X_2 = 1$ for the parallel polarity alignment, which is expected from the identical nominal geometry designs of the two STVOs.

Table I lists the fitting results along with the microwave field amplitude h_{rf} . In all cases the mean of phase-locking amplitudes is proportional to the microwave field. For the antiparallel polarity alignment, the extracted dipolar coupling Ω slightly increases with h_{rf} . One reason is that the vortex gyration amplitude X_i might be increased as STVO i is phase-locked to the microwave field, resulting in an enhancement of Ω_{ij} on STVO j . Another possibility is the incomplete phase locking at small h_{rf} (observed in Fig. 3a for STVO 2)

due to thermal fluctuations, which are likely to reduce the effective coupling. Owing to these two counteracting effects, we take the average of the three experiments, $\Omega_{AP} = -8.0$ MHz, as the extracted value of Ω . For the parallel polarity alignment, the level of frequency pulling is similar to Fig. 3(b) but the frequency mismatch between the two STVOs is much smaller. We thus expect a smaller coupling strength Ω_P compared to Ω_{AP} . From the fitting we extract $\Omega_P = 3.6$ MHz which is 2.2 times smaller than $|\Omega_{AP}|$. We point out that the ratio between the two dipolar coupling strengths agrees with the ratio of critical frequency mismatch, $\Delta f_{AP}/\Delta f_P = 2.4$ found in our prior work[17], and depends on the exact geometry of the STVOs pair[39].

The phase shift γ_i^{NL} is determined by the position of the largest frequency pulling in Fig. 3. In the antiparallel polarity alignment the values of γ_i^{NL} are reproducible at various microwave fields but differ from that in the parallel alignment, indicating large variations of parameters in magnetic dynamics upon polarity change. From the model we interpret $\tan \gamma_i^{NL}$ as the reduced nonlinear coefficient ν_i of STVO i [48]. However we note that the fitting results with negative values of γ_i^{NL} point towards more complex dynamics than assumed in the simple analytical model.

DISCUSSION

Our results provide a versatile experimental approach to study coupled oscillators with an external ac drive. With controllable phase between the ac source and one phase-locked oscillator, we acquire not only the amplitude but also the phase information of the inter-device coupling. This probing technique is not restricted to spin-torque oscillators and microwave field, but applicable to all coupled oscillator systems and ac drives.

As an application, we show that two dipolarly coupled STVOs follow ideal oscillator systems described by Eq. (1), a pre-assumption for studies based on the Kuramoto model[53]. We confirm that the dipolar coupling strength can be tuned by a factor greater than two with bistable polarity states[17, 39], providing a unique freedom to manipulate the collective dynamics. In addition we learn about the nonlinearities in STVOs. Finite phase lags γ_i^{NL} are measured, as predicted in theory[48, 54] and identified in similar systems[18, 27]. By setting $\Delta_{ie} = 0$, Eq. (1) describes Sakaguchi-Kuramoto-model behaviors[20]: with nonzero γ_i^{NL} the system can fall into incoherent states at medium Ω but is barely influenced at large Ω . We also point out that with $\gamma_i^{NL} = 0$ attracting and repulsive interactions will be present for the two different polarity alignments, with which a new propagating wave mode has been predicted[55]. Nevertheless the natural nonlinearity in devices will always mediate the two extremes.

One interesting finding is that the extracted Ω in the antiparallel polarity alignment is much smaller than the phase-locking frequency mismatch of 28 MHz found in Fig. 1(g). From the analysis above we deduce nearly identical amplitude ratio. In the phase-locking solution derived by Slavin and Tiberkevich[56], the maximal frequency mismatch for mutual synchronization in this case is $\Omega(\nu_1 + \nu_2)$. Thus we confirm the role of nonlinearities, with $\nu_1 + \nu_2$ around 3.5, in the large phase-locking frequency mismatch. The fact that the synchronized mode is closer to the peak branch of STVO 1 likely indicates that ν_2 is greater than ν_1 , making it easier for STVO 2 to adapt its frequency to STVO 1.

In summary, we have developed a novel approach to study two coupled auto-oscillators. In the presence of an external microwave field, we show that two STVOs can exhibit additional frequency pulling due to dipolar coupling. Fittings to an analytical model show tunable dipolar coupling strength Ω by controlling the relative polarity alignment and finite phase lag γ_i^{NL} for practical oscillators. These results thus extend the understanding of coupled oscillator systems which are useful for further investigations of collective dynamics in larger arrays of auto-oscillators.

We thank R. Lebrun, V. V. Naletov and A. N. Slavin for fruitful discussions. We acknowledge the MEMOS project ANR-14-CE26-0021 for financial support.

* yi.li@cea.fr

† gregoire.deloubens@cea.fr

- [1] A. Pikovsky and M. Rosenblum, *CHAOS* **25**, 097616 (2015).
- [2] K. Wiesenfeld, P. Colet, and S. H. Strogatz, *Phys. Rev. Lett.* **76**, 404 (1996).
- [3] S.-B. Shim, M. Imboden, and P. Mohanty, *Science* **316**, 95 (2007).
- [4] G. Heinrich, M. Ludwig, J. Qian, B. Kubala, and F. Marquardt, *Phys. Rev. Lett.* **107**, 043603 (2011).
- [5] M. Zhang, G. S. Wiederhecker, S. Manipatruni, A. Barnard, P. McEuen, and M. Lipson, *Phys. Rev. Lett.* **109**, 233906 (2012).
- [6] S. Kaka, M. R. Pufall, W. H. Rippard, T. J. Silva, S. E. Russek, and J. A. Katine, *Nature* **437**, 389 (2005).
- [7] F. B. Mancoff, N. D. Rizzo, B. N. Engel, and S. Tehrani, *Nature* **437**, 393 (2005).
- [8] I. Z. Kiss, Y. Zhai, and J. L. Hudson, *Science* **296**, 1676 (2002).
- [9] M. R. Tinsley, S. Nkomo, and K. Showalter, *Nat. Phys.* **8**, 662 (2012).
- [10] L. H. Hartwell, J. J. Hopfield, S. Leibler, and A. W. Murray, *Nature* **402**, C47 (1999).
- [11] N. Locatelli, V. Cros, and J. Grollier, *Nat. Mater.* **13**, 11 (2013).
- [12] J. Grollier, D. Querlioz, and M. D. Stiles, *Proc. IEEE* **104**, 2024 (2016).
- [13] Y. Kuramoto, *Chemical Oscillations, Waves, and Turbulence* (Springer, Beilin, 1984).

- [14] J. A. Acebrón, L. L. Bonilla, C. J. Pérez-Vicente, F. Ritort, and R. Spigler, *Rev. Mod. Phys.* **77**, 137 (2005).
- [15] A. Ruotolo, V. Cros, B. Georges, A. Dussaux, J. Grolier, C. Deranlot, R. Guillemet, K. Bouzehouane, S. Fusil, and A. Fert, *Nature Nano.* **4**, 528 (2009).
- [16] S. Sani, J. Persson, S. M. Mohseni, Y. Pogoryelov, P. K. Muduli, A. Eklund, G. Malm, M. Käll, A. Dmitriev, and J. Åkerman, *Nature Comm.* **4**, 2731 (2013).
- [17] N. Locatelli, A. Hamadeh, F. Abreu Araujo, A. D. Belanovsky, P. N. Skirdkov, R. Lebrun, V. V. Naletov, K. A. Zvezdin, M. Muñoz, J. Grolier, O. Klein, V. Cros, and G. de Loubens, *Sci. Rep.* **5**, 17039 (2015).
- [18] R. Lebrun, S. Tsunegi, P. Bortolotti, H. Kubota, A. S. Jenkins, M. Romera, K. Yakushiji, A. Fukushima, J. Grolier, S. Yuasa, and V. Cros, *arXiv*, 1601.01247 (2016).
- [19] V. Tiberkevich, A. Slavin, E. Bankowski, and G. Gerhart, *Appl. Phys. Lett.* **95**, 262505 (2009).
- [20] O. E. Omel'chenko and M. Wolfrum, *Phys. Rev. Lett.* **109**, 164101 (2012).
- [21] S. I. Kiselev, J. C. Sankey, I. N. Krivorotov, N. C. Emley, R. J. Schoelkopf, R. A. Buhrman, and D. C. Ralph, *Nature* **425**, 380 (2003).
- [22] W. H. Rippard, M. R. Pufall, S. Kaka, T. J. Silva, S. E. Russek, and J. A. Katine, *Phys. Rev. Lett.* **95**, 067203 (2005).
- [23] B. Georges, J. Grolier, M. Darques, V. Cros, C. Deranlot, B. Marcihac, G. Faini, and A. Fert, *Phys. Rev. Lett.* **101**, 017201 (2008).
- [24] S. Urzhidyn, P. Tabor, V. Tiberkevich, and A. Slavin, *Phys. Rev. Lett.* **105**, 104101 (2010).
- [25] M. Quinsat, J. F. Sierra, I. Firastrau, V. Tiberkevich, A. Slavin, D. Gusakova, L. D. Buda-Prejbeanu, M. Zarudniev, J.-P. Michel, U. Ebels, B. Dieny, M.-C. Cyrille, J. A. Katine, D. Mauri, and A. Zeltser, *Appl. Phys. Lett.* **98**, 182503 (2011).
- [26] A. Hamadeh, N. Locatelli, V. V. Naletov, R. Lebrun, G. de Loubens, J. Grolier, O. Klein, and V. Cros, *Appl. Phys. Lett.* **104**, 022408 (2014).
- [27] R. Lebrun, A. Jenkins, A. Dussaux, N. Locatelli, S. Tsunegi, E. Grimaldi, H. Kubota, P. Bortolotti, K. Yakushiji, J. Grolier, A. Fukushima, S. Yuasa, and V. Cros, *Phys. Rev. Lett.* **115**, 017201 (2015).
- [28] V. S. Pribiag, I. N. Krivorotov, G. D. Fuchs, P. M. Braganca, O. Ozatay, J. C. Sankey, D. C. Ralph, and R. A. Buhrman, *Nature Phys.* **3**, 498 (2007).
- [29] A. Dussaux, B. Georges, J. Grolier, V. Cros, A. V. Khvalkovskiy, A. Fukushima, M. Konoto, H. Kubota, K. Yakushiji, S. Yuasa, K. A. Zvezdin, K. Ando, and A. Fert, *Nature Commun.* **1**, 8 (2010).
- [30] N. Locatelli, V. V. Naletov, J. Grolier, G. de Loubens, V. Cros, C. Deranlot, C. Ulysse, G. Faini, O. Klein, and A. Fert, *Appl. Phys. Lett.* **98**, 062501 (2011).
- [31] A. Hamadeh, N. Locatelli, V. V. Naletov, R. Lebrun, G. de Loubens, J. Grolier, O. Klein, and V. Cros, *Phys. Rev. Lett.* **112**, 257201 (2014).
- [32] V. Sluka, A. Kákay, A. M. Deac, D. E. Bürgler, M. Schneider, C. and R. Hertel, *Nat. Comm.* **6**, 6409 (2015).
- [33] J. Shibata, K. Shigeto, and Y. Otani, *Phys. Rev. B* **67**, 224404 (2003).
- [34] S. Sugimoto, Y. Fukuma, S. Kasai, T. Kimura, A. Barman, and T. Otani, *Phys. Rev. Lett.* **106**, 197203 (2011).
- [35] D.-S. Han, A. Vogel, H. Jung, K.-S. Lee, M. Weigand, H. Stoll, G. Schütz, P. Fischer, G. Meier, and S.-K. Kim, *Sci. Rep.* **3**, 2262 (2013).
- [36] A. D. Belanovsky, N. Locatelli, P. N. Skirdkov, F. Abreu Araujo, J. Grolier, K. A. Zvezdin, V. Cros, and A. K. Zvezdin, *Phys. Rev. B* **85**, 100409(R) (2012).
- [37] A. D. Belanovsky, N. Locatelli, P. N. Skirdkov, F. Abreu Araujo, K. A. Zvezdin, J. Grolier, V. Cros, and A. K. Zvezdin, *Appl. Phys. Lett.* **103**, 122405 (2013).
- [38] F. Abreu Araujo and J. Grolier, *J. Appl. Phys.* **120**, 103903 (2016).
- [39] F. Abreu Araujo, A. D. Belanovsky, P. N. Skirdkov, K. A. Zvezdin, A. K. Zvezdin, N. Locatelli, R. Lebrun, J. Grolier, V. Cros, G. de Loubens, and O. Klein, *Phys. Rev. B* **92**, 045419 (2015).
- [40] G. Csaba, M. Pufall, D. Nikonov, G. Bourianoff, A. Horvath, T. Roska, and W. Porod, in *Cellular Nanoscale Networks and Their Applications (CNNA), 2012 13th International Workshop on* (2012) pp. 1–2.
- [41] D. E. Nikonov, G. Csaba, W. Porod, T. Shibata, D. Voils, D. Hammerstrom, I. A. Young, and G. I. Bourianoff, *IEEE Journal on Exploratory Solid-State Computational Devices and Circuits* **1**, 85 (2015).
- [42] See the Supplemental Information for details.
- [43] A. V. Khvalkovskiy, J. Grolier, N. Locatelli, Y. V. Gorbunov, K. A. Zvezdin, and V. Cros, *Appl. Phys. Lett.* **96**, 212507 (2010).
- [44] V. V. Naletov, G. de Loubens, G. Albuquerque, S. Borlenghi, V. Cros, G. Faini, J. Grolier, H. Hurdequint, N. Locatelli, B. Pigeau, A. N. Slavin, V. S. Tiberkevich, C. Ulysse, T. Valet, and O. Klein, *Phys. Rev. B* **84**, 224423 (2011).
- [45] G. de Loubens, A. Riegler, B. Pigeau, F. Lochner, F. Boust, K. Y. Guslienko, H. Hurdequint, L. W. Molenkamp, G. Schmit, A. V. Slavin, V. S. Tiberkevich, N. Vukadinovic, and O. Klein, *Phys. Rev. Lett.* **102**, 177602 (2009).
- [46] A. Dussaux, A. V. Khvalkovskiy, P. Bortolotti, J. Grolier, V. Cros, and A. Fert, *Phys. Rev. B* **86**, 014402 (2012).
- [47] K. Y. Guslienko, B. A. Ivanov, V. Novosad, Y. Otani, H. Shima, and K. Fukamichi, *J. Appl. Phys.* **91**, 8037 (2002).
- [48] A. Slavin and V. Tiberkevich, *IEEE Trans. Magn.* **45**, 1875 (2009).
- [49] K. Y. Guslienko, *Appl. Phys. Lett.* **89**, 022510 (2006).
- [50] B. A. Ivanov and C. E. Zaspel, *Phys. Rev. Lett.* **99**, 247208 (2007).
- [51] A. V. Khvalkovskiy, J. Grolier, A. Dussaux, K. A. Zvezdin, and V. Cros, *Phys. Rev. B* **80**, 140401(R) (2009).
- [52] R. Adler, *Proc. IRE* **34**, 351 (1973).
- [53] V. Flovik, F. Macià, and E. Wahlström, *Sci. Rep.* **6**, 32528 (2016).
- [54] J. Persson, Y. Zhou, and J. Åkerman, *J. Appl. Phys.* **101**, 09A503 (2007).
- [55] H. Hong and S. H. Strogatz, *Phys. Rev. Lett.* **106**, 054102 (2011).
- [56] A. N. Slavin and V. S. Tiberkevich, *Phys. Rev. B* **74**, 104401 (2006).